

# DEVELOPMENT OF DEEP CHARGE MONITORING SYSTEM FOR SPACECRAFT UTILIZING THE PIPWP METHOD

Watanabe, R., Tanaka, H., Tanaka, Y., Takada, T., Murooka, Y. and Tomita, N.

Department of Mechanical Systems Engineering

Musashi Institute of Technology

1-28-1, Tamazutsumi, Setagaya-ku, Tokyo, 158-8557, JAPAN

TEL/FAX : +81-3-5707-1187

E-mail : [rwata@eng.musashi-tech.ac.jp](mailto:rwata@eng.musashi-tech.ac.jp)

## Abstract

Equipment for measurement of internal charges in dielectric materials has been developed in order to apply it for spacecrafts as a real time charge monitoring system. A non-destructive and direct measurement technique, called PIPWP method, is utilized to observe charge distribution of dielectrics in bulk. This method also enables us to measure the charge accumulating process in real time. The measurement results clarified the charge accumulating/dissipating process in a PMMA film during/after electron beam irradiation for 5 minutes. The distributions of the electric field and the electric potential were also calculated. A spacecrafts' onboard charge monitoring system concept is outlined and it was found that we needed further modification to put it in practice.

## Introduction

Spacecraft Charging has been thought as one of most possible causes of spacecraft failures because it induces degradation of dielectrics, anomalies or breakdown of on-board electronics<sup>[1]</sup>. Although NASA has been conducting thorough investigations on charging related phenomena since 1970s, spacecraft anomalies, which are caused by spacecraft charging, still exist<sup>[2]</sup>. It means that we need further understandings on charging related phenomena and improvements for preventing the failures and anomalies.

Most of studies carried out in the past focused on Surface Charging which occurs on the surface of a spacecraft in low energy plasma environment because it was thought that it caused surface discharges<sup>[3]</sup>. Recently, however, it has been pointed out that there is possibility that Internal Charging is related somehow to discharging of spacecraft besides surface charging<sup>[4]</sup>.

Measurement systems for surface charging have been well established and successful for over 30 years. On the other hand, deep charges are difficult to measure by the existing techniques. Thus, nobody has tried direct measurement of charged particles in dielectric materials used on spacecraft.

We succeed in developing a new type of deep charge monitor system<sup>[5]</sup> which utilized a PIPWP (Piezo-electric Induced Pressure Wave Propagation) method<sup>[6]</sup> recently. It enables us measuring charge distribution directly and continuously in real time. We measured the charge distribution in a PMMA (Polymethyl Methacrylate) film during/after electron beam irradiation (230 keV). The results showed that the electron beam penetrates the sample at about 300  $\mu$ m under the irradiated surface. The results of the experiment are summarized in this paper.

Based on this achievement, we are planning to install this measurement system on a small experimental satellite to be launched in 2005. This satellite, SERVIS (Space Environment Reliability Verification Integrated System), is being developed to verify commercial off-the-shelf parts and technologies in the severe space environment so that they can be utilized for space applications. In verifying them, precise information of space environment is required and thus a measurement system which are consist of particle detector, monitors for SEU (Single Event Upset)/SEL (Single Event Latch-up)/TD (Total Dose) are to be installed.

Our system, however, was developed for the use under atmospheric condition and needs to be modified to sustain the space environments. In this paper, the onboard charge monitoring system concept is outlined and required modifications are discussed.

## PIPWP Method

The PIPWP method is applied to our system. Principle of the PIPWP method is shown in Fig. 1. The pulsed pressure wave  $p(t)$  acts as a charge probe. When there are electric charges  $\rho(z)$  in the sample, the position of charges will be moved slightly by the pressure wave, then the movement of the charges induces the change of surface charges on the electrode. The differential of surface charge ( $dq(t)/dt$ ) causes a displacement current  $i(t)$  in the external circuit.

The time history of the displacement current indicates the charge distribution in the sample. The detected displacement current is given by equation (1) which is expressed by convolution integral, where  $\rho_{sa}$  is density of the sample,  $u_{sa}$  is acoustic velocity in the sample,  $a$  is thickness of the sample,  $Z_{sa}$  and  $Z_{Al}$  are acoustic impedances of the sample and aluminum respectively.

$$i(t) = \frac{A}{\rho_{sa} u_{sa} a} \frac{2Z_{sa}}{Z_{sa} + Z_{Al}} \times \left[ \sigma(0)p(t) + u_{sa} \int_0^{\infty} \rho(\tau)p(t-\tau)d\tau + \sigma(a)p(t-a/u_{sa}) \right] \quad (1)$$

### Measurement System

Figure 2 shows the system diagram of the measurement system. It consists of “Pulse generator”, “Sensor”, “Power supply”, “Digitizing oscilloscope” and “Computer”. The pulse generator supplies a pulsed voltage (200V, 400ns) to the piezo-electric transducer (PVDF 9 $\mu$ m) in order to generate a pulsed pressure wave propagating toward the sample. The electric signal that is measured in the sensor is taken into digital oscilloscope and the data is sent to computer. Computer controls all the system so that the real-time and continuous measurements of the charge distributions are carried out during/after the irradiation.

Figure 3 shows a schematic diagram of the sensor. The electron beam irradiates the sample within the hole ( $\phi 6\text{mm}$ ) on the top. Both surfaces of the sample and the glass are aluminum coated in order to ground the top surface of the sample and the bottom surface of the glass. Therefore, the bottom of the sample is floated and it is where the electric signal is acquired. The dimension of the sensor is 89mm(W) 54mm(D) 50mm(H) and the weight is 400g.

### Electron Beam Irradiation Experiment

We tried to measure the charge accumulation and deposition process inside a dielectric sample (PMMA) of 510  $\mu\text{m}$  thickness. Figure 4 shows a schematic diagram of the irradiation equipment. Electrons are accelerated in the vacuum space with the acceleration voltage of 230 keV. The sensor is placed in the atmospheric space filled with  $\text{N}_2$  gas for

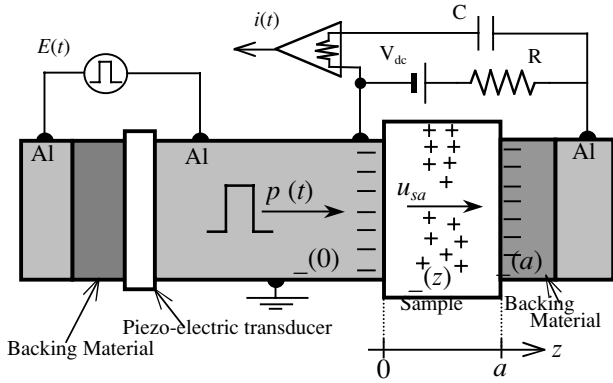


Fig. 1. Principle of PIPWP method

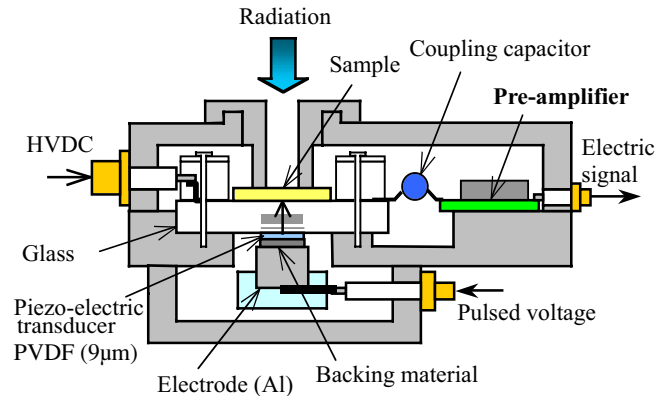


Fig. 3. Sensor

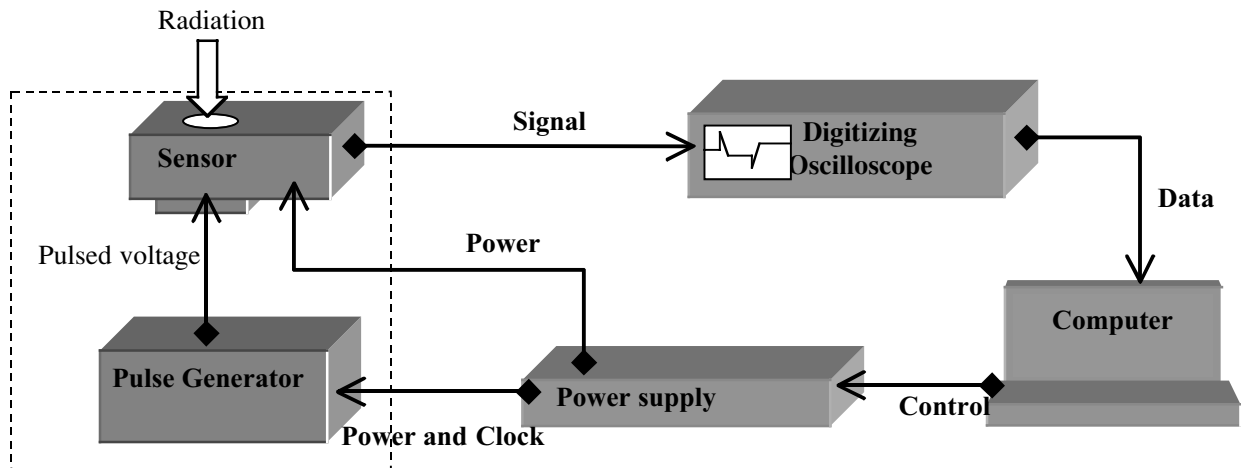


Fig. 2. The system diagram of the PIPWP method

cooling. Between the two spaces, there is a Titanium foil where the accelerated electrons are passing through. Irradiation with current density  $10 \text{ } [\mu\text{A}/\text{cm}^2]$  lasts for 5 minutes. The intervals of data acquisition are 10 sec. And the computer processes the data with a deconvolution program on LabVIEW.

## Experimental Results

### (1) Charge distribution

The observed charge accumulation process in the PMMA sample is shown in Fig. 5. The horizontal axis indicates the perpendicular distance along the sample, and the vertical axis indicates the charge density  $\rho(z)$ . The sample is in between the electrodes that those interfaces exist at 0 and  $510 \text{ } \mu\text{m}$  in the horizontal axis. The distributions are plotted in each 30 seconds from -30 s to 5 min. The electron beam irradiates from right to left as indicated in the figure. Note that two peaks at the interfaces ( $0 \text{ } \mu\text{m}$  and  $510 \text{ } \mu\text{m}$ ) are positive charges that are induced by the negative charges inside the sample. It is interesting to know that the charges start to accumulate “evenly” in the region between the irradiated surface and a certain depth ( $315 \text{ } \mu\text{m}$  in this test). Subsequently, they start to have a peak around  $220 \text{ } \mu\text{m}$  from the surface. This is because the electrons accumulated near the surface are gradually attracted by the increasing positive charges induced at the irradiated surface. Thus, only the charges near the negative peak can continue to accumulate. Another interesting observation is that the rate of accumulation is decreasing as it goes on and it seems that it is going to saturate and reach an equilibrium state. At the end of irradiation, though we did not continue until it is fully saturated, the maximum peak charge density is  $-33 \text{ } \mu\text{C}/\text{cm}^3$  at  $220 \text{ } \mu\text{m}$  from the irradiated surface. The maximum penetration depth, which depends on the acceleration voltage, does not change during the irradiation.

Regarding the resolution of these results, they have resolution of  $31 \text{ } \mu\text{m}$  in the irradiation direction. It is decided by the input pulse width and the cut-off frequency of the Gaussian filter that cuts the high frequency noise. Narrowing the pulse width naturally improves the measurement accuracy, but it requires a high performance pulse generator and high voltage, which is difficult to supply in satellite systems. Conversely, it means that you can adjust the accuracy of the measurement system as required.

After the irradiation, we continued to measure the charge distribution in the sample in order to clarify the dissipation process of the accumulated charges. Figure 6 shows the results. They are of 0, 5, 10, 20, 30 minutes after the irradiation. It is found that the charges are dissipating rapidly near the peak but some remained even 30 minutes after the irradiation. It indicates that once the electrons are accumulated in a dielectric material, there exists some residual charge even if the irradiation terminated. Another interesting observation in this figure is that the charges close to the interface (electrode) are dissipating more rapidly than that accumulated in deeper location. This might be related to the electric field distribution and will be discussed later.

### (2) Electric field distribution

From the charge distributions, the electric field distributions can be calculated by integrating the Poisson's equation along the  $z$  direction.

$$-\frac{\rho(z)}{\epsilon} = -\frac{\partial E(z)}{\partial z} = \frac{\partial^2 V(z)}{\partial z^2} \quad (2)$$

Where  $\rho(z)$  is charge density [ $\text{C}/\text{cm}^3$ ],  $\epsilon$  is dielectric constant of the sample,  $E(z)$  is electric field,  $V(z)$  is electric potential and  $z$  is the direction of thickness of the sample.

The calculated distributions of the electric field are plotted in Fig. 7. The electric field intensity grows up as the charges are accumulating especially near the irradiated surface. Around the charge peak, however, it is weaker than that of the other region. Thus, the electrons coming “uniformly” into the sample are affected by the strong electric field so that the charge distributions have a peak inside the sample as shown in Fig. 5. At the end of the irradiation, the maximum intensity of the electron field reaches  $-990 \text{ kV}/\text{cm}$ , which appears near the irradiated surface.

The electric field distributions are also calculated after the irradiation as shown in Fig. 8. The intensity of the electric field decays as the charges are dissipating. There exist remaining electric field of  $\pm 400 \text{ kV}/\text{cm}$  even 30 minutes

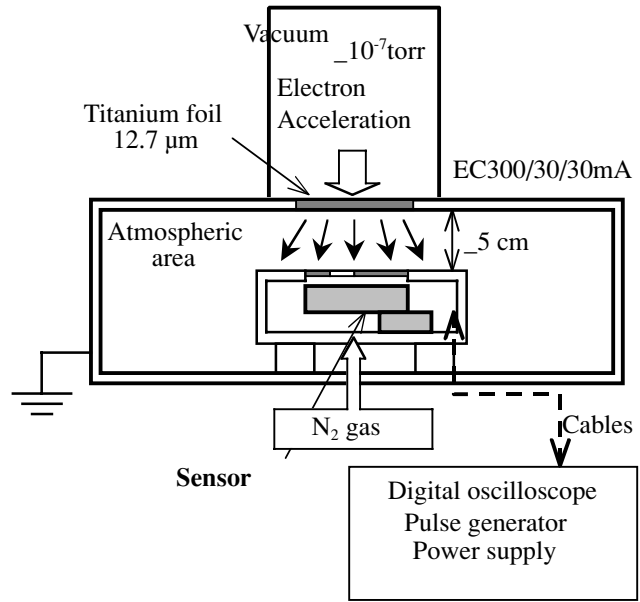


Fig. 4. Electron beam irradiation equipment

after the irradiation.

One explanation for the reason why the charges close to the electrode dissipating more rapidly is that such electrons are affected intensely by the strong electric field built up near the electrode as shown in this figure. Therefore, they move quickly and the charge decay rapidly. On the other hand, charges trapped in deeper location move slowly because there exist weaker electric field near the charge peak.

Another possible explanation is that the electric conductivity becomes larger near the irradiated surface and it results in rapid dissipation of charges close to it. On the other hand, the charges in deeper location are difficult to move because the conductivity around there does not change.

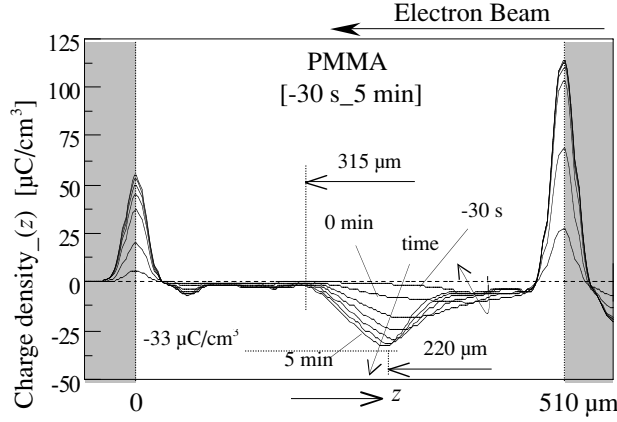


Fig. 5. Charge distribution in PMMA during electron beam irradiation

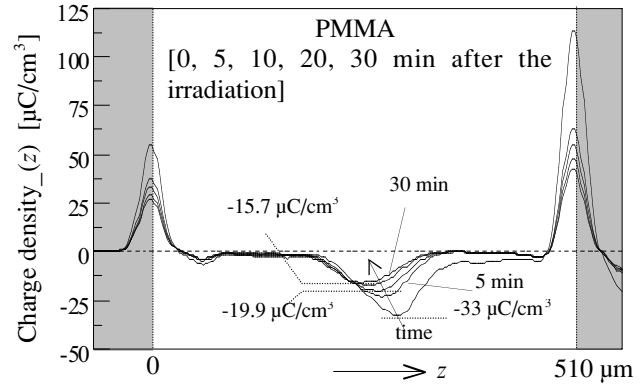


Fig. 6. Charge distribution in PMMA after electron beam irradiation

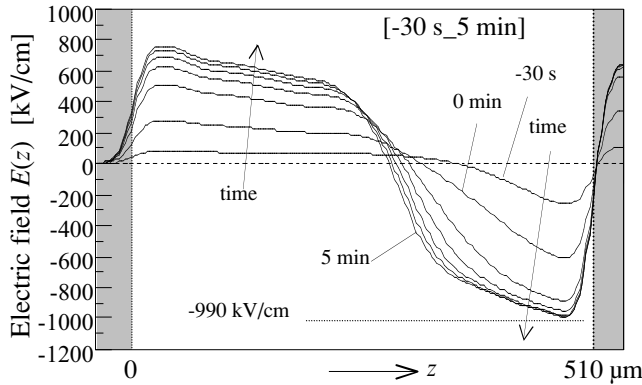


Fig. 7. Electric Field distribution in PMMA during irradiation electron beam

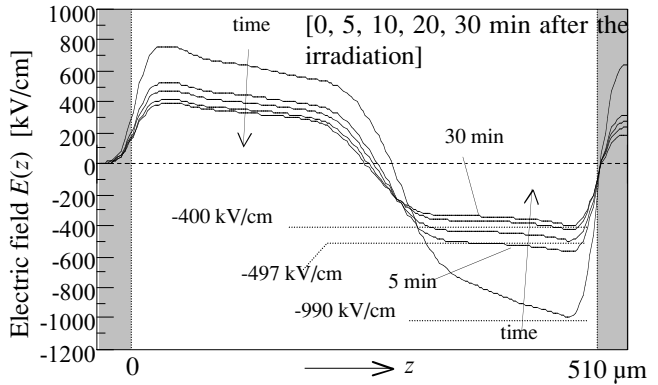


Fig. 8. Electric field distribution in PMMA after electron beam irradiation

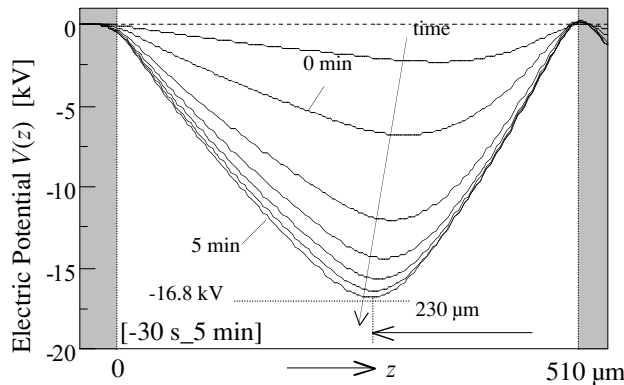


Fig. 9. Electric potential distribution in PMMA during irradiation electron beam

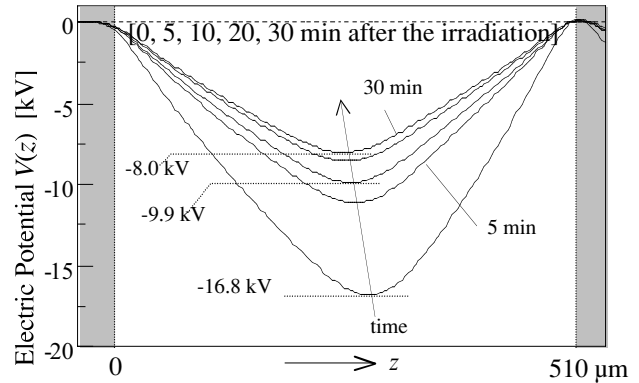


Fig. 10. Electric potential distribution in PMMA after electron beam irradiation

### (3) Electric potential distribution

The electric potential distributions during/after the irradiation can be calculated by integrating the electric field distributions in the z direction. Figure 9 shows the variation of the electric potential distributions during the irradiation. They clearly show how the electric potential is increasing during the electron irradiation. It is interesting to know that the peak of the electric potential moves slightly from where it was at the start of the irradiation according to the charge up process. At the end of the irradiation, the maximum strength of the electric potential is -16.8 kV at the depth of 230  $\mu\text{m}$  from the irradiated surface.

The electric potential distributions are also calculated after the irradiation as shown in Fig. 10. As the same reason mentioned above, the potential peak moves slightly toward the deeper location. Even 30 minutes after the irradiation, the peak value of the potential remains to be -8.0 kV.

Although the charge distributions are successfully measured in real-time, we need to conduct through experiments especially on the following subjects in order to clarify the charge up mechanism inside dielectric materials.

- (a) Relation between the charge peak location and the acceleration voltage
- (b) Dependency of temperature on the charge accumulation/dissipation process
- (c) Effect of electric density to the total amount of the accumulated charges
- (d) Vacuum environment

These investigations would be a great help for understanding and modeling the charge/discharge phenomena.

## Onboard Charge Monitoring System

As shown in above, we have succeeded in developing the deep charge measurement system and some interesting observations are obtained from the electron beam irradiation experiment.

Based on this achievement, we have been planning to install this system onto a Japanese satellite in order to put it into practical use. Our system, however, was designed for the use under the atmospheric environment as a first step. Thus, we need to modify the whole system so that it can be used under the space environment.

In this section, the specifications of the satellite system are outlined, and the improvement of our measurement system is discussed. The experimental results of out gassing tests recently conducted are also shown.

### (1) SERVIS satellite

The satellite system we have been thinking of is called SERVIS (Space Environmental Reliability Verification Integrated System) #2 satellite that is to be launched in 2005. This system was planned to verify commercial off-the-shelf parts and technologies in the severe space environment so that they can be utilized for space applications. Using low cost parts and technologies will drastically reduce the cost of satellite systems.

For verifying these parts, a space environmental monitoring system that measures the actual environment parts will experience is needed. Thus, several monitors such as a single event upset monitor, a total dose monitor, a light particle monitor and surface/bulk charge monitors will be onboard. We are going to make a proposal for this satellite system so that our system is adopted as a bulk charge sensor.

### (2) Design modification

The most important thing we must take care is the material selection that will affect the outgassing and contamination characteristics. Presently, acrylic plastics are used for holding the glass as shown in Fig. 3 and they are to be replaced with fluoroplastics. Vinyl coated cables inside the sensor are also replaced with Teflon coated cables. The whole electric circuit (pre amplifier) will be potted.

The remaining problem we have to overcome is the use of silicon grease that is laying between the glass and the sample. Since the pressure wave propagating through the glass and the sample acts as a charge probe in the PIPWP method, the interfaces should be connected tightly so that the pressure wave could transmit them without attenuation.

We tested the outgassing characteristics of the silicon grease and the PMMA, which is currently used as the sample. Table 1 shows the experimental result. The test is conducted at NASDA Space Center (Tsukuba) and it is compliant with the ASTM E595-93. As shown in this table, CVCM of the silicon grease exceeds 0.1 %, which is the criterion of NASA. Thus, we cannot use the silicon grease

Table 1 Outgassing data of materials

Material	TML[%]	CVCM [%]	WVR [%]
PMMA	0.563	0.000	0.468
Silicon grease	0.852	<u>0.140</u>	0.034

for the onboard sensor. An alternative way to establish the firm contact is simply adhering between the glass and the sample. However, we have not found any adhesives appropriate for our usage.

Another thing we have to consider is the interface with the satellite. If the charge distributions inside the sample are measured continuously, huge storage and high-speed data processing system are required. However, if we use this equipment as a alarm device for accumulated charges, required accuracy for the charge distributions will be eased and this results in lesser storage and simpler measurement system.

### **Summary**

Measurement equipment using PIPWP method for investigating spacecraft internal charging was developed successfully. We measured charge distributions in dielectrics sample (PMMA) during/after the electron beam irradiation in the atmosphere. The experimental results clarified the charge accumulation/dissipation processes inside the sample and showed some characteristic as follows. (1) The charge build up occurs at a certain location that is affected by the acceleration voltage. (2) Some charges still remain inside the sample after the irradiation stops.

The electric field distributions and the electric potential distributions are also calculated. As a result, it was found that strong electric fields are induced near the interfaces and the high electric potential builds up at the charge peak.

We have shown the only test case but we need through researches such as on dependency of the acceleration voltage, temperature, the current density and vacuum. These investigations will contribute to analysis on the charge up mechanism and the discharge characteristics.

The outline of SERVIS satellite on which our equipment will be installed as a charge monitor is shown and the design modifications to our measurement system are briefly summarized. More detailed specifications are working out currently.

### **Acknowledgement**

This study is carried out as a part of "Ground Research Announcement for Space Utilization" promoted by Japan Space Forum. The authors wish to acknowledge the assistance of NASDA Tsukuba Research Center on execution of the outgassing tests.

### **Reference**

- [1] H. B. Garrett : Rev. Geophys. Space Phys, 19 (1981) pp. 577.
- [2] C. K. Purvis, H. B. Garrett and N. J. Stevens : Handbook of Design Guidelines for Assessment and Controlling Spacecraft Charging Effects, NASA TP-2361, 1984.
- [3] H. Nishimoto, H. Fujii and T. Abe : Observation of Surface Charging on Engineering Test Satellite \_ of Japan, AIAA 89-0613, 1989.
- [4] N. John Stevens : Spacecraft Charging Study of A GEO Communications Satellite, AIAA 98-0984, 1998.
- [5] H. Tanaka and N. Tomita : "Development of Measurement System for Bulk Charge Distribution in Dielectrics in Space Environment," The International Symposium on Space Technology and Science, ISTS 2000-s-11, May 2000.
- [6] Tatsuo Takada : "Acoustic and Optical Method for Measuring Electric Charge Distributions in Dielectrics." WHITEHEAD MEMORIAL, *IEEE Transaction on Dielectrics and Electrical Insulation*, Vol. 6 No. 5, October 1999, pp. 519-547.